T.&A.M. Report No. 462

Analysis of Wire Ropes with Internal-Wire-Rope Cores

James W. Phillips
Professor

George A. Costello
Professor, Fellow ASME

Department of Theoretical and Applied Mechanics
University of Illinois at Urbana-Champaign
Urbana, IL 61801

Abstract

Stresses in the individual wires of complex wire rope are determined for rope constructions having an internal-wire-rope core (IWRC). The ropes may be pulled, twisted, and bent over a sheave or drum. Specific results for 6x19 Seale IWRC and 6x25 filler-wire IWRC ropes that are prevented from twisting indicate that the maximum stresses (exclusive of contact stresses) are typically 1.5 to 3 times as large as the nominal rope stress based on rope load and total metallic area.

Introduction

Over the years, many types of wire rope have been designed and tested for various applications where a tensile load must be transmitted by a flexible member. In spite of the long time that wire rope has been in use, relatively little theoretical work has appeared on the analysis of stresses in the individual wires of complex wire rope. Suslov [1] even states that "a mathematical calculation of the stresses (in wire rope) by the theory of elasticity is impossible, owing to a great number of unknown changeable units . . . ." On the other hand, the results of extensive testing programs involving both static and fatigue loading have been reported. In 1945, Drucker and Tachau [2] assessed the existing fatigue data and presented a useful design criterion for wire rope.

In the early 1950's, Hall [3] and Hruska [4-6] developed some of the first theoretical models to predict the stresses in the individual wires of a strand. Leissa [7], Starkey and Cress [8], and Bert and Stein [9] also pursued the problem of predicting stresses in a strand. Durelli and Machida [10,11] combined experimental and analytical methods to investigate the behavior of strands. The axial stresses in armor wires of bent submarine cables (strands) were the subject of investigation in a 1969 paper by Lutchansky [12]. Recently, Knapp [13] reexamined the problem of armored cables (strands). Huang [14] has investigated the finite extension of an elastic strand with a central core wire.

In 1973, the authors published a paper on the contact stresses in a strand [15]; in the paper the six nonlinear equations of equilibrium for a thin wire were solved for the case of a wire initially in the shape of a helix. This solution led to a series of papers [16-22] wherein various properties of a strand were investigated.

Velinsky [23] made a major contribution in 1981, when he linearized the theory developed by Costello et al., and provided a rational procedure for treating the strands in a rope in a manner not unlike that for treating wires within a strand. In particular, Velinsky considered the Seale construction with an internal-wire-rope core (IWRC), as shown in Fig. 1.

Important aspects of Velinsky's work were subsequently discussed in a paper by Velinsky, Anderson and Costello [24] wherein the theory is compared with experiment. Phillips and Fotsch [25] later presented similar results for a particular filler-wire construction that is commonly used in hoisting operations.

The purpose of this paper is to generalize the approach developed by Velinsky [23] for any kind of wire rope that contains an IWRC. Expressions for the axial, bending, torsional, and line-contact loads on individual wires and on the strands that comprise complex wire-rope constructions are developed for the common loading situation where a rope is pulled axially and simultaneously bent over a sheave or drum. The results for several types of rope are presented in a nondimensional form that allows the relative merits of different types of rope to be determined quantitatively.

Analysis of a straight rope

The analysis of a rope begins with a study of the deformation of a helical wire in a straight strand. By "piecing together" the deformations of all the wires in a given strand, one determines the axial and torsional response of that strand. Each strand in the rope is then assumed to have been bent into the shape of a helix, and, again by "piecing together" the deformations of all the strands in the rope, one determines the axial and torsional response of a straight rope; in this last step, the bending stiffness of each strand is taken to be the sum of the bending stiffnesses of the individual wires in that strand.

General relations for a wire or strand

The equations of equilibrium for a helical wire in a straight strand are the same as those for a helical strand in a straight rope. In either case, the relevant equations can be derived from Love's general equilibrium equations [26] for an arbitrarily shaped thin rod undergoing small extensional strain, namely:

$$\frac{dN}{d\xi} - N'\tau + T\kappa' + X = 0, \tag{1}$$

$$\frac{dN'}{d\xi} - T\kappa + N\tau + Y = 0, \tag{2}$$

$$\frac{dT}{d\xi} - N\kappa' + N'\kappa + Z = 0, \tag{3}$$

$$\frac{dG}{d\xi} - G'\tau + H\kappa' - N' + K = 0, \tag{4}$$

$$\frac{dG'}{d\xi} - H\kappa + G\tau + N + K' = 0, \tag{5}$$

$$\frac{dH}{d\xi} - G\kappa' + G'\kappa + \Theta = 0, \tag{6}$$

where ξ denotes the position along the wire or strand centerline; N, N' and T denote the normal and binormal shear forces and the tensile force, respectively; G, G' and H denote the normal and binormal bending moments and the twisting moment, respectively; κ, κ' and τ denote the normal and binormal curvatures and the twist, respectively, in the deformed state; X, Y and Z denote externally applied distributed forces per unit length in the normal, binormal and tangential directions, respectively; and K, K' and Θ denote externally applied distributed moments per unit length in the normal, binormal and tangential directions, respectively. See Fig. 2.

When a helical wire or strand is deformed into the shape of another helix, the normal curvature κ vanishes in both the initial and final configurations. If it is assumed (1) that G

vanishes if κ undergoes no change, (2) that G' and H depend only on κ' and τ, (3) that T, κ' and τ are independent of ξ, and (4) that $K = 0$ and $K' = 0$, then equations (1−6) will be satisfied if and only if $Y = 0$, $Z = 0$, $N = 0$, $\Theta = 0$, and:

$$X = N'\tau - T\kappa', \tag{7}$$

where

$$N' = -G'\tau + H\kappa'. \tag{8}$$

Strictly speaking, these equations for X and N' are nonlinear since τ and κ' refer to the deformed configuration of the wire or strand [15]; however, in the work presented here, the changes in τ and κ' during deformation are very small, and with sufficient accuracy, the values of τ and κ' in the equilibrium equations (7) and (8) may be taken to be the initial values.

Analysis of a wire

Consider first the deformation of a helical wire in a *straight* strand that is pulled and twisted. The strand is to be regarded as any one of the m_s strands in the sth strand layer in the rope. Within this strand there are l_s layers of helically wrapped wires; the ith layer of these wires contains m_{si} identical wires, each having the wire radius R_{si}, the helix angle α_{si} (measured counter-clockwise from a plane normal to the strand centerline—see Fig. 2), and the helix radius r_{si}. In the initial configuration, the normal and binormal curvatures and twist of each wire are given by

$$\kappa_{si} = 0, \quad \kappa'_{si} = \frac{\cos^2\alpha_{si}}{r_{si}}, \quad \text{and} \quad \tau_{si} = \frac{\sin\alpha_{si}\cos\alpha_{si}}{r_{si}}, \tag{9}$$

respectively. When the strand is pulled and twisted, each wire undergoes an axial (extensional) strain ϵ_{si}, in addition to changes $\Delta\kappa'_{si}$ and $\Delta\tau_{si}$ in the binormal curvature and twist, respectively. There is no change in the normal curvature. The nonvanishing

generalized strains (ϵ_{si}, $\Delta\kappa'_{si}$, $\Delta\tau_{si}$) give rise to the generalized wire loads

$$T_{si} = \pi R_{si}^2 \epsilon_{si}, \tag{10}$$

$$G'_{si} = \frac{\pi E R_{si}^4}{4} \Delta\kappa'_{si}, \tag{11}$$

and

$$H_{si} = \frac{\pi E R_{si}^4}{4(1+\nu)} \Delta\tau_{si}. \tag{12}$$

Since there is no change in the normal curvature, the normal bending moment G_{si} is equal to zero. In equations (10−12), E and ν denote Young's modulus and Poisson's ratio, respectively, for the wire material.

Small changes in r_{si} and α_{si} are directly related to small changes in curvature and twist, and *vice versa*. It is readily shown by partial differentiation of equations (9) that

$$r_{si}\,\Delta\tau_{si} = -\frac{\cos\alpha_{si}\sin\alpha_{si}}{r_{si}}\Delta r_{si} + (\cos^2\alpha_{si} - \sin^2\alpha_{si})\,\Delta\alpha_{si} \tag{13a}$$

and

$$r_{si}\,\Delta\kappa'_{si} = -\frac{\cos^2\alpha_{si}}{r_{si}}\Delta r_{si} - 2\cos\alpha_{si}\sin\alpha_{si}\,\Delta\alpha_{si}. \tag{13b}$$

Equations (13) may be inverted to give

$$\frac{\Delta r_{si}}{r_{si}} = -2\tan\alpha_{si}\,(r_{si}\Delta\tau_{si}) + (\tan^2\alpha_{si} - 1)\,(r_{si}\Delta\kappa'_{si}) \tag{14a}$$

and

$$\Delta\alpha_{si} = (r_{si}\Delta\tau_{si}) - \tan\alpha_{si}\,(r_{si}\Delta\kappa'_{si}). \tag{14b}$$

The reason for performing the inversion is that the changes in helix radius and helix angle will appear in subsequent calculations, whereas the generalized strains in the wire are taken to be ϵ_{si}, $\Delta\tau_{si}$ and $\Delta\kappa'_{si}$.

Compatibility conditions for wires within a strand

A straight strand that is pulled and twisted undergoes an axial strain ϵ_s and a change in twist (angle of twist per unit length) $\Delta\tau_s$. The wire layers comprising the strand must deform in a manner compatible with these strand strains, and, in addition, adjacent wire layers must remain in contact with each other.

In all, three "compatibility conditions" arise for each layer of wires. The first two are found by considering the extension and the change in twist, respectively, of the strand. It is easily shown [17] that when a given wire undergoes an extensional strain ϵ_{si} and a change in helix angle $\Delta\alpha_{si}$, the strand must undergo an axial strain ϵ_s satisfying the condition

$$(1+\epsilon_{si})\,\sin(\alpha_{si}+\Delta\alpha_{si}) \;=\; (1+\epsilon_s)\,\sin\alpha_{si}, \tag{15}$$

where no restriction is placed on the magnitudes of ϵ_{si}, ϵ_s and $\Delta\alpha_{si}$. For small changes in these variables, however, equation (15) may be linearized, with the result that

$$\epsilon_s \;=\; \epsilon_{si} + \cot\alpha_{si}\,\Delta\alpha_{si}. \tag{16}$$

In view of equation (14b), this result may also be stated in the form

$$\epsilon_s \;=\; \epsilon_{si} + \cot\alpha_{si}\,(r_{si}\Delta\tau_{si}) - (r_{si}\Delta\kappa'_{si}). \tag{17}$$

Similarly, it may be shown [17] that the change in strand twist $\Delta\tau_s$ satisfies the nonlinear relation

$$\frac{\cos\alpha_{si}}{r_{si}} + \sin\alpha_{si}\,\Delta\tau_s \;=\; \frac{(1+\epsilon_{si})\,\cos(\alpha_{si}+\Delta\alpha_{si})}{r_{si}+\Delta r_{si}}, \tag{18}$$

where $\Delta\tau_s$, ϵ_{si}, $\Delta\alpha_{si}$ and Δr_{si} may be arbitrarily large; for small values of these variables, however, equation (18) becomes

$$\Delta\tau_s \;=\; \frac{1}{r_{si}}\left[\cot\alpha_{si}\left(-\frac{\Delta r_{si}}{r_{si}}+\epsilon_{si}\right)-\Delta\alpha_{si}\right], \tag{19}$$

which in view of equations (14) is equivalent to the relation

$$r_{si}\,\Delta\tau_s \;=\; \cot\alpha_{si}\,\epsilon_{si} + (r_{si}\,\Delta\tau_{si}) + \cot\alpha_{si}\,(r_{si}\,\Delta\kappa'_{si}). \tag{20}$$

Equations (17) and (20) provide two conditions that the values of ϵ_{si}, $\Delta\tau_{si}$ and $\Delta\kappa'_{si}$ must satisfy. The necessary third condition for wires in the ith wire layer of a given strand is that they remain in contact with the wires in some other layer—usually the $(i-1)$th layer—in the same strand. Consider, for example, the wires in a regular-lay 6x19 Seale IWRC, as shown in Fig. 3. There are three layers of strands; the first two layers ($s = 1,2$) comprise the internal-wire-rope core, and the third layer ($s = 3$) consists of the six outer Seale strands. Careful measurement of the wires in the innermost IWRC strand ($s = 1$) reveals that a wire in the second layer ($i = 2$) touches the center wire ($i = 1$) and *not* the neighboring second-layer wires, i.e. the helix radius of the "12" wires is simply

$$r_{12} \;=\; R_{11} + R_{12}.$$

Similarly, it is found that $r_{22} = R_{21} + R_{22}$ for the outer wires of the core's outer strands, and that, in the Seale strand, $r_{32} = R_{31} + R_{32}$ for the nine intermediate-layer wires. The outermost wires of the Seale strand are nested between those of the intermediate layer; it is easily shown that, if the wire cross sections are approximated by circles, then

$$r_{33} \;=\; \cos(\pi/9)\,R_{31} + [\cos(\pi/9) + \cos\gamma]\,R_{32} + \cos\gamma\,R_{33},$$

where

$$\gamma \;=\; \arcsin\left[\frac{R_{31}+R_{32}}{R_{32}+R_{33}}\sin(\pi/9)\right].$$

Note that the helix radii r_{si} are always of the form

$$r_{si} \;=\; \sum_{j=1}^{i} \eta_{sij}\,R_{sj}, \tag{21}$$

where the η_{sij} are known dimensionless weighting factors of the order of unity. For all the types of rope considered in this paper, either the η_{sij} are pure constants (such as 0 or 1), or they are complicated but *extremely weak* functions of the helix angle α_{si}, in which case the

functions may be approximated by constants evaluated under the assumption that the wire cross sections are circular. A change in helix radius Δr_{si} will then be attributed only to Poisson contraction of all the wires in the strand, i.e.

$$r_{si} + \Delta r_{si} = \sum_{j=1}^{i} \eta_{sij} (1 - \nu \epsilon_{sj}) R_{sj}, \tag{22}$$

or

$$\Delta r_{si} = \Delta r_{si}^{p} - \nu \eta_{sii} R_{si} \epsilon_{si}, \tag{23a}$$

where Δr_{si}^{p}, which is defined as

$$\Delta r_{si}^{p} = -\nu \sum_{j=1}^{i-1} \eta_{sij} R_{sj} \epsilon_{sj}, \tag{23b}$$

is that part of Δr_{si} that is due to the Poisson contraction of wires in layers beneath the ith layer. If the ϵ_{sj} for $j = 1, \cdots, i-1$ have already been calculated, then Δr_{si}^{p} is a known quantity.

In view of equation (14a), the result in equation (23a) may be stated as

$$\frac{1}{r_{si}} \Delta r_{si}^{p} = \frac{1}{r_{si}} \nu \eta_{sii} R_{si} \epsilon_{si} + 2 \tan \alpha_{si} (r_{si} \Delta \tau_{si}) + (\tan^2 \alpha_{si} - 1) (r_{si} \Delta \kappa'_{si}). \tag{24}$$

Multiplying this equation by $\cot^2 \alpha_{si} / r_{si}$, and recalling equations (17) and (20), one can now write the following set of linear equations for the unknowns ϵ_{si}, $\Delta \tau_{si}$ and $\Delta \kappa'_{si}$:

$$\begin{bmatrix} 1 & \cot \alpha_{si} & -1 \\ \cot \alpha_{si} & 1 & \cot \alpha_{si} \\ \nu \eta_{sii} (R_{si}/r_{si}) \cot^2 \alpha_{si} & -2 \cot \alpha_{si} & (1 - \cot^2 \alpha_{si}) \end{bmatrix} \begin{Bmatrix} \epsilon_{si} \\ r_{si} \Delta \tau_{si} \\ r_{si} \Delta \kappa'_{si} \end{Bmatrix} = \begin{Bmatrix} \epsilon_{s} \\ r_{si} \Delta \tau_{s} \\ (\cot^2 \alpha_{si} / r_{si}) \Delta r_{si}^{p} \end{Bmatrix}. \tag{25}$$

In the often encountered case where a wire is parallel to the strand axis, i.e. $\cot \alpha_{si} = 0$, equations (25) yield $\epsilon_{si} = \epsilon_{s}$, $\Delta \tau_{si} = \Delta \tau_{s}$, and $\Delta \kappa'_{si} = 0$. In general, however, $\cot \alpha_{si} \neq 0$ and equations (25) are solved by some appropriate method, such as Cramer's rule.

Generalized forces on a strand

The resultant tensile force T_s on a strand is given by

$$T_s = \sum_{i=1}^{l_s} m_{si} \, (T_{si} \sin\alpha_{si} + N'_{si} \cos\alpha_{si}), \tag{26}$$

while the resultant torque H_s is given by

$$H_s = \sum_{i=1}^{l_s} m_{si} \, [(H_{si} \sin\alpha_{si} + G'_{si} \cos\alpha_{si}) + r_{si} \, (T_{si} \cos\alpha_{si} - N'_{si} \sin\alpha_{si})], \tag{27}$$

where T_{si}, G'_{si}, H_{si} and N'_{si} are computed from equations (10,11,12,8), respectively, after the values of ϵ_{si}, $\Delta\tau_{si}$ and $\Delta\kappa'_{si}$ for all the wires in the strand have been determined by solving equations (25) for $i = 1, \cdots, l_s$.

A value for the strand binormal bending moment resultant G'_s will be needed in subsequent calculations. If it is assumed that the wires in a strand are free to slide relative to each other, then the bending stiffness of the strand will be equal to the sum of the bending stiffnesses of the individual wires comprising the strand, i.e. [27,28]

$$G'_s = \left(\sum_{i=1}^{l_s} m_{si} \, \frac{\sin\alpha_{si}}{1 + \frac{1}{2}\nu \cos^2\alpha_{si}} \, \frac{\pi E R^4}{4} \right) \Delta\kappa'_s, \tag{28}$$

where $\Delta\kappa'_s$ is the change in curvature of the strand centerline. McConnell and Zemke's recent experimental results for complex strands [29] seem to indicate that this assumption is a reasonable one for well-lubricated rope.

Strand geometry

A rope is formed from strands in a manner that greatly resembles the manner in which the strands are formed from wires. One complicating feature of strand response within a rope, however, is that the deformed radius of a strand depends not only on the axial strain of

the strand, but also on the change in twist of the strand; this matter will be discussed after some preliminary remarks are made about the initial strand geometry.

Typical IWRC ropes contain three layers of strands—two layers that comprise the IWRC and a third layer consisting of strands of a particular type, such as a Seale, Warrington, filler-wire, or flattened strand. The initial helix radii of the strands in a rope are usually easy to specify in terms of the radii of the strands, since strands are seldom "nested" among themselves. Let R_s be the radius of the sth strand. If the l_s layers of wires in this strand have been ordered in such a way that the l_sth layer of wires is the outermost one, then

$$R_s = r_{si} + R_{si} \quad (i = l_s \text{ only}). \tag{29}$$

The helix radius r_s of the sth strand will be of the form

$$r_s = \sum_{t=1}^{s} \eta_{0st} R_t, \tag{30}$$

where, typically, the constants η_{0st} are integers. Consider the 6x19 Seale IWRC in Fig. 3 again as an example. Here it is noted that

$$r_1 = 0, \quad r_2 = R_1 + R_2, \quad \text{and} \quad r_3 = R_1 + 2R_2 + R_3,$$

i.e.

$$\eta_{011} = 0; \quad \eta_{021} = 1, \quad \eta_{022} = 1; \quad \text{and}$$

$$\eta_{031} = 1, \quad \eta_{032} = 2, \quad \eta_{033} = 1.$$

Finally, the rope radius R can be calculated by noting that it is equal to the helix radius of the outermost strand plus the radius of that strand, i.e.

$$R = r_s + R_s \quad (s = l \text{ only}). \tag{31}$$

Each preformed strand in a rope has its own twist τ_s and curvature κ'_s given by

$$\tau_s = \frac{\sin\alpha_s \cos\alpha_s}{r_s} \quad \text{and} \quad \kappa'_s = \frac{\cos^2\alpha_s}{r_s}, \tag{32a,b}$$

where α_s is the helix angle of that strand within the rope. When the rope is subjected to an axial force T and twisting moment H, each strand in the rope is subjected to an axial strain ϵ_s and changes in the strand twist and curvature, denoted by $\Delta\tau_s$ and $\Delta\kappa'_s$, respectively.

Compatibility conditions for strands within a rope

As was the case for wires within a strand, there arise three conditions governing the behavior of strands within a rope, and these three conditions lead to a set of three simultaneous equations for the generalized strand strains ϵ_s, $\Delta\tau_s$ and $\Delta\kappa'_s$. The first two conditions are similar those encountered previously for wires within a strand, and lead to the expressions

$$\epsilon = \epsilon_s + \cot\alpha_s (r_s \Delta\tau_s) - (r_s \Delta\kappa'_s) \tag{33}$$

and

$$r_s \Delta\tau = \cot\alpha_s \epsilon_s + (r_s \Delta\tau_s) + \cot\alpha_s (r_s \Delta\kappa'_s), \tag{34}$$

where ϵ and $\Delta\tau$ are, respectively, the axial strain and the change in twist, respectively, of the rope.

The third condition pertains to the change in strand radius. This change must occur in such a way that strands in the sth strand layer remain in contact with those in the $(s-1)$th strand layer. Recall that the original strand radius R_s is given by equations (21,29), i.e.

$$R_s = \sum_{j=1}^{i} \eta_{sij} R_{sj} + R_{si} \qquad (i = l_s \text{ only}),$$

which may be written more compactly as

$$R_s = \sum_{j=1}^{l_s} \eta_{s0j} R_{sj}, \tag{35a}$$

where

$$\eta_{s0j} \equiv \begin{cases} \eta_{sij}, & i = l_s \text{ and } j \neq l_s \\ \eta_{sij}+1, & i = l_s \text{ and } j = l_s \end{cases}. \tag{35b}$$

A change in strand radius ΔR_s will satisfy the relation

$$R_s + \Delta R_s = \sum_{j=1}^{l_s} \eta_{s0j} (1-\nu\epsilon_{sj}) R_{sj}, \tag{36}$$

where the ϵ_{sj} are the strains in the individual wires, i.e.

$$\Delta R_s = -\nu \sum_{j=1}^{l_s} \eta_{s0j} \epsilon_{sj} R_{sj}. \tag{37}$$

It is important to note that both the extension and the twisting of a strand give rise to strains ϵ_{sj} in the individual wires of a strand, and consequently both modes of loading must be considered when computing the change in strand radius. The fact that the twisting of a strand affects the radius of the strand is one of the features that distinguishes the behavior of a strand from that of a solid wire.

Since the ϵ_{sj} are linear functions of both ϵ_s and $\Delta\tau_s$, and since the ϵ_{sj} vanish when both ϵ_s and $\Delta\tau_s$ are equal to zero, it follows that

$$\epsilon_{sj} = \frac{\partial\epsilon_{sj}}{\partial\epsilon_s}\epsilon_s + \frac{\partial\epsilon_{sj}}{\partial\Delta\tau_s}\Delta\tau_s, \tag{38}$$

where the partial derivatives $\partial\epsilon_{sj}/\partial\epsilon_s$ and $\partial\epsilon_{sj}/\partial\Delta\tau_s$ can be computed (numerically if necessary) from the previously developed solution for wires within a loaded strand. Using equation (38), one can rewrite equation (37) in the form

$$\Delta R_s = \frac{\partial R_s}{\partial\epsilon_s}\epsilon_s + \frac{\partial R_s}{\partial\Delta\tau_s}\Delta\tau_s, \tag{39}$$

where

$$\frac{\partial R_s}{\partial \epsilon_s} = -\nu \sum_{j=1}^{l_s} \eta_{s0j} \frac{\partial \epsilon_{sj}}{\partial \epsilon_s} R_{sj} \quad \text{and}$$
$$\frac{\partial R_s}{\partial \Delta\tau_s} = -\nu \sum_{j=1}^{l_s} \eta_{s0j} \frac{\partial \epsilon_{sj}}{\partial \Delta\tau_s} R_{sj} \tag{40}$$

are the *known* derivatives for all strands up to and including the sth one.

One can now return to equation (30) and note that the change in strand helix radius Δr_s must satisfy the equation

$$r_s + \Delta r_s = \sum_{t=1}^{s} \eta_{0st} (R_s + \Delta R_t), \tag{41}$$

that is, with the aid of equation (39),

$$\Delta r_s = \Delta r_s^p + \eta_{0ss} \frac{\partial R_s}{\partial \epsilon_s} \epsilon_s + \eta_{0ss} \frac{\partial R_s}{\partial \Delta\tau_s} \Delta\tau_s, \tag{42}$$

where Δr_s^p denotes that portion of Δr_s that is due solely to the known changes in strand radii of strands underlying the sth one:

$$\Delta r_s^p \equiv \sum_{t=1}^{s-1} \eta_{0st} \left(\frac{\partial R_t}{\partial \epsilon_t} \epsilon_t + \frac{\partial R_t}{\partial \Delta\tau_t} \Delta\tau_t \right). \tag{43}$$

Equation (42) will now be transformed so that the variables describing the strand's deformation will be the same as those used in equations (33,34). This is done by recalling a fundamental relation—similar to equation (14a)—that gives the change in helix radius Δr_s as a function of the change in twist $\Delta\tau_s$ and the change in curvature $\Delta\kappa_s'$. Performing this substitution, multiplying both sides of the resulting equation by $\cot^2\alpha_s / r_s$, and introducing the definitions

$$C_s^{\epsilon} \equiv \eta_{0ss} \frac{\partial R_s}{\partial \epsilon_s}, \qquad C_s^{\Delta\tau} \equiv \eta_{0ss} \frac{\partial R_s}{\partial \Delta\tau_s}, \tag{44a,b}$$

one finds that

$$-\frac{\cot^2\alpha_s}{r_s}C_s^{\epsilon}\epsilon_s+[-2\cot\alpha_s-\frac{\cot^2\alpha_s}{r_s}C_s^{\Delta\tau}](r_s\Delta\tau_s)+(1-\cot^2\alpha_s)(r_s\Delta\kappa'_s)=\frac{\cot^2\alpha_s}{r_s}\Delta r_s^p \quad (45)$$

Three independent linear equations have now been derived for the generalized strains ϵ_s, $\Delta\tau_s$ and $\Delta\kappa'_s$ associated with the sth strand: equations (33) and (34), which ensure that the strand will deform in a manner compatible with that of the rope, and equation (45), which ensures that the various layers of strands will remain in contact with each other in the deformed configuration of the rope. The three equations, when collected together, are:

$$\begin{bmatrix} 1 & \cot\alpha_s & -1 \\ \cot\alpha_s & 1 & \cot\alpha_s \\ -(\cot^2\alpha_s/r_s)C_s^{\epsilon} & -2\cot\alpha_s-(\cot^2\alpha_s/r_s)C_s^{\Delta\tau} & (1-\cot^2\alpha_s) \end{bmatrix}\begin{Bmatrix} \epsilon_s \\ r_s\Delta\tau_s \\ r_s\Delta\kappa'_s \end{Bmatrix}=\begin{Bmatrix} \epsilon \\ r_s\Delta\tau \\ (\cot^2\alpha_s/r_s)\Delta r_s^p \end{Bmatrix}. \quad (46)$$

These equations governing strands in a rope are nearly identical in form to equations (25), which govern the individual wires in a strand. In fact, if one merely rewrites the third of equations (25) as

$$-\frac{\cot^2\alpha_{si}}{r_{si}}C_{si}^{\epsilon}\epsilon_{si}+[-2\cot\alpha_{si}-\frac{\cot^2\alpha_{si}}{r_{si}}C_{si}^{\Delta\tau}](R_{si}\Delta\tau_{si})+(1-\cot^2\alpha_{si})(r_{si}\Delta\kappa'_{si})=\frac{\cot^2\alpha_{si}}{r_{si}}\Delta r_{si}^p$$

and sets

$$C_{si}^{\epsilon}=-\nu\eta_{sii}R_{si} \quad \text{and} \quad C_{si}^{\Delta\tau}=0,$$

then the forms of equations (25) and (46) *will* be identical. This last observation effects a certain simplification in computer programming.

Having solved equations (46) for each strand in the rope, one can use equations (26−28) to determine the tensile force T_s, the twisting moment H_s, and the bending moment G'_s acting on each strand. Equilibrium equations (7,8) can then be used to determine the shear force N'_s and the distributed normal load X_s acting on each strand:

$$N_s' = H_s\kappa_s' - G_s'\tau_s \quad \text{and}$$
$$X_s = N_s'\tau_s - T_s\kappa_s', \tag{47}$$

where τ_s and κ_s' are the twist and curvature of the sth strand, given by equations (32).

The total force T and twisting moment H sustained by the rope can now be computed by resolving in the axial direction of the rope the forces and moments acting on individual strands. The process is analogous to the procedure used for each strand, in terms of the wires within the strands—see equations (26,27)—and the results are:

$$T = \sum_{s=1}^{l} m_s\,(T_s \sin\alpha_s + N_s' \cos\alpha_s) \tag{48}$$

and

$$H = \sum_{s=1}^{l} m_s\,[(H_s \sin\alpha_s + G_s' \cos\alpha_s) + r_s\,(T_s \cos\alpha_s - N_s' \sin\alpha_s)], \tag{49}$$

where m_s is the number of strands in the sth layer of strands, and l is the number of strand layers.

Concluding remarks

A general procedure has been outlined for determining the axial, bending, shear, torsional, and distributed normal loads on each wire, and on each strand of wires, in a straight IWRC rope containing an arbitrary number of layers of strands, each strand containing an arbitrary number of layers of wires. Poisson contraction of individual wires is accounted for. The rope may be given an arbitrary axial strain ϵ and an arbitrary twist $\Delta\tau$. All equations are linear, and the maximum number of simultaneous equations to be solved at any stage of the procedure is three.

Analysis of loaded rope bent over a sheave

The preceding analysis has dealt with a rope that remains straight in its loaded configuration; a boom pendant is an example of such a rope. Most rope, however, is cyclically subjected not only to axial loads but also to additional bending loads that are induced when the rope is would around a drum or passed over a sheave, as illustrated in Fig. 4.

It is recognized that an "exact" analysis of the deformation of a loaded rope passed over a sheave would be exceedingly complex, especially if an attempt were made to analyze in detail the transition regions where the rope enters and leaves the sheave. In this paper, it will be assumed that the stresses in the individual wires of an axially loaded rope bent around a sheave consist of the stresses that would exist in the same axially loaded rope if it were straight, *plus* the bending stresses that would be induced in the individual preformed wires, each in the shape of a double helix, bent elastically into the rope-centerline curvature that is imposed by the sheave. Except perhaps for questions concerning the redistribution of wire loads within the transition regions, one can argue that this assumption is a reasonable one for well-lubricated rope.

It can be shown [28] that the maximum change in normal curvature $\Delta\kappa_{si}$ in a helical wire in a straight strand that is undergoing a change in strand curvature $\Delta\kappa_s$ has a value somewhat smaller than that of $\Delta\kappa_s$, namely

$$\Delta\kappa_{si} = \frac{\sin\alpha_{si}}{1+\frac{1}{2}\nu\cos^2\alpha_{si}}\,\Delta\kappa_s, \tag{50}$$

where α_{si} is the helix angle of the wire within the strand. Similarly, the maximum change in strand curvature $\Delta\kappa_s$ that occurs when the axis of a straight strand is bent into the arc of a circle of radius $D/2$ is

$$\Delta\kappa_s = \frac{\sin\alpha_s}{1+\frac{1}{2}\nu_s\cos^2\alpha_s}\cdot\frac{1}{D/2}, \tag{51}$$

where α_s is the helix angle of the strand in the rope, and ν_s is a "strand Poisson's ratio." The term $\frac{1}{2}\nu_s\cos^2\alpha_s$ has a magnitude much smaller than unity and with negligible error ν_s may be set equal to the Poisson's ratio of the wire material, ν. Equations (31,50,51) may now be used to predict the maximum bending stress σ_{si}^B due to sheave curvature in terms of the D/d ratio, where d is the rope diameter (equal to $2R$), as follows:

$$\begin{aligned}\sigma_{si}^B &= ER_{si}\Delta\kappa_{si} \\ &= E\frac{R_{si}}{R}\frac{\sin\alpha_s}{1+\frac{1}{2}\nu\cos^2\alpha_s}\cdot\frac{\sin\alpha_{si}}{1+\frac{1}{2}\nu\cos^2\alpha_{si}}\left(\frac{D}{d}\right)^{-1}.\end{aligned} \tag{52}$$

The factors involving $\sin\alpha_s$ and $\sin\alpha_{si}$ vary between about 0.9 and 1 for typical rope constructions. The appearance of the factor R_{si}/R in equation (52) suggests that, for a given D/d ratio, the stresses due to bending over a sheave or drum can be minimized by using a rope having a large number of very fine wires, as is generally well known.

Results and Discussion

The geometrical data for some of the ropes that have been considered appear in Table 1. The data for "solid rod", "1x7 strand", and "7x7 lang lay" are actually those for the center wire, the central strand, and the entire IWRC, respectively, of a $1\frac{1}{4}$-in. (32 mm) Seale IWRC, which is also listed. The last entry is for a $\frac{1}{2}$-in. (13 mm) 6x25 filler-wire IWRC. Note that the Seale and the filler-wire ropes are both of regular lay, although the lays are of opposite sense.

Results for straight rope

For each rope listed in Table 1, the generalized strains and loads in each wire and strand in the rope have been calculated for an overall rope strain ϵ of 1000 $\mu\epsilon$ and a rope twist $\Delta\tau$ of zero. The results are listed in Table 2. (Although the analysis developed in this paper allows the rope twist $\Delta\tau$ to take on nonzero values, most rope in service is prevented from rotating—at least at its ends—during use; consequently results for nonzero $\Delta\tau$ will not be reported here.) Young's modulus E for the wire material is taken as 30.0×10^6 psi (207 GPa).

In Table 2, the column headings ϵ, $\Delta\tau$, $\Delta\kappa'$, T, etc., are understood to have the subscripts s or si when entries for strands or wires are considered. Note that the maximum axial strains ϵ_s and ϵ_{si} occur in strands and wires that are aligned with the rope axis; the axial strains in all other wires are smaller in magnitude. On the other hand, the wires that are not axially aligned within strands sustain changes in curvature and twist and are therefore subjected to bending and shear stresses that the axially aligned wires do not experience.

As it turns out, the shearing stresses due to the twisting moments H_{si} and the transverse shear forces N'_{si} are negligible, at least in the present case where $\Delta\tau = 0$. The maximum tensile stress on the cross section of a given wire, due to the axial extension of a straight rope, is given by

$$\sigma_{si}^{T} = \frac{1}{\pi R_{si}^2} T_{si} + \frac{R_{si}}{\pi R_{si}^4/4} |G'_{si}| + \frac{ER_{si}\sin\alpha_{si}}{1+\frac{1}{2}\nu\cos^2\alpha_{si}} |\Delta\kappa'_s|, \tag{53}$$

where the last term arises because of the bending stresses induced in strand wires when the strand undergoes a change in curvature—see equation (28). Although the binormal axis of a wire within a strand does not generally coincide with the binormal axis of the strand, these axes will coincide once within each lay length of the wire within the strand, and consequently the algebraic addition of the maximum bending stresses in equation (53) is justifiable if one is seeking only the maximum stresses in a given wire cross section.

The line loads X_s and X_{si} give rise to contact stresses that can be very large [15,16], but

no attempt is made to calculate values of the contact stresses in this paper. It should be mentioned that the X_s and X_{si} values given in Table 2 are *net* values of the distributed line loads and may be due to contact with wires or strands both in layers inside and in layers outside a given wire or strand layer.

The data in Table 2 may be scaled for ropes of identical construction but of different rope diameter d. Force resultants vary as d^2 whereas moment resultants vary as d^3. Thus, if the loads T and H for a $1\frac{1}{4}$-in. (32 mm) 6x25 filler-wire IWRC rope are desired for a rope strain ϵ of 1000 $\mu\epsilon$ with no twist, they become simply $T = (1.25/0.50)^2 \times 2835 = 17{,}700$ lbf (78.8 kN), and $H = (1.25/0.50)^3 \times (-120) = -1880$ lbf-in (-212 N·m). Note that these values do not differ significantly from those for the Seale IWRC of the same rope diameter; the "restraining torque" H is of opposite sign in the two cases because the ropes are of opposite lay.

It is interesting to compute the values of σ_{si}^T in equation (53) and to compare them with the nominal stress σ_{nom} defined by

$$\sigma_{\text{nom}} \equiv \frac{T}{A}, \tag{54}$$

where A is the "metallic area" of the rope:

$$A = \sum_{s=1}^{l} m_s \sum_{i=1}^{l_s} m_{si} \pi R_{si}^2. \tag{55}$$

The nondimensional ratio, or "straight rope factor",

$$z_{si}^T \equiv \frac{\sigma_{si}^T}{\sigma_{\text{nom}}} \tag{56}$$

is given in Table 2 for all the wires in the various ropes under consideration. Note that this ratio is always greater than or equal to unity. Actually, it suffices to compare just the term $E\epsilon_{si}$ (the leading term in equation (53)) with the term $E_{\text{eff}}\epsilon$, where E_{eff} is the effective modulus [17] of the rope, to see why this is so. The effective modulus is given by

$$E_{\text{eff}} \equiv \frac{\sigma_{\text{nom}}}{\epsilon} = \frac{T}{A\epsilon} \tag{57}$$

and turns out to have the values $1.00E$, $0.889E$, $0.798E$, $0.702E$ and $0.762E$, respectively, for the five ropes listed in Table 2. The values of ϵ_{si} are consistently greater than $(E_{\text{eff}}/E)\epsilon$ and thus the axial wire stresses consistently exceed the nominal rope stress.

Worn-in ropes containing an IWRC are known to have an effective modulus of about one-half [30] to two-thirds of E in the "working region" of the load-deflection curve. Since the present theory does not account for the radial deformation due to the point and line loads associated with the X_s and X_{si}, the theory should be providing an upper bound on the effective modulus. This seems to be the case.

Loaded rope bent over a sheave or drum

When a straight rope sustaining a nominal stress σ_{nom} is bent around a drum or sheave of diameter D, additional bending stresses given by equation (52) are imposed. By superposition, the maximum stress σ_{si} in an arbitrary wire may be represented in a nondimensional form as

$$\frac{\sigma_{si}}{\sigma_{\text{nom}}} = z_{si}^{T} + z_{si}^{B}\left(\frac{D}{d}\cdot\frac{\sigma_{\text{nom}}}{E}\right)^{-1}, \tag{58}$$

where, from equation (52), the "bending factor" z_{si}^{B} is given by

$$z_{si}^{B} = \frac{R_{si}}{R}\cdot\frac{\sin\alpha_s}{1+\frac{1}{2}\nu\cos^2\alpha_s}\cdot\frac{\sin\alpha_{si}}{1+\frac{1}{2}\nu\cos^2\alpha_{si}}. \tag{59}$$

Values of z_{si}^{B} are given in Table 2. It should be noted that both z_{si}^{T} and z_{si}^{B} are independent of E and σ_{nom}. When σ_{si} is normalized with respect to σ_{nom}, the value of σ_{nom} appears in the parameter multiplying z_{si}^{B} because the bending stresses due to sheave curvature are actually independent of σ_{nom}.

Recommended values of D/d for headframe sheaves lie between about 60 and about

100, depending on the rope diameter, the rope construction, and the type of application [31], and σ_{nom} is typically of the order of $0.003E$, at least for steel rope with the usual factors of safety applied. Maximum values of the parameter $\frac{D}{d} \cdot \frac{\sigma_{nom}}{E}$ are therefore of the order of 0.3, as illustrated in Fig. 5, where the normalized maximum stresses in the 6x25 filler-wire IWRC are plotted in accordance with equation (58) and the appropriate values of z_{si}^{T} and z_{si}^{B} from Table 2.

Note that, for large values of $\frac{D}{d} \cdot \frac{\sigma_{nom}}{E}$, it is the centermost wire of the IWRC which is subjected to the maximum stress; this stress is approximately $1.5\sigma_{nom}$ even for *very large* values of D/d. On the other hand, for values of $\frac{D}{d} \cdot \frac{\sigma_{nom}}{E}$ less than about 0.1, it is the center wire of the filler-wire strand that experiences the maximum stress, which becomes arbitrarily large as $D/d \rightarrow 0$; maximum-stress values of 2 or 3 times σ_{nom} would be typical for rope which is wrapped around small sheaves (as in the case of the various hoist ropes in mobile yard cranes). In the filler-wire rope, the small filler wire itself is understressed throughout the loading range. All the other wires, however, are stressed in a remarkably uniform manner. It is perhaps this uniformity in stress loading that has led to the widespread use of filler-wire rope in hoisting operations.

A comparison between the Seale and the filler-wire constructions can be made by examining the values of z_{si}^{T} and z_{si}^{B} in Table 2. The central strand of the IWRC of the Seale rope has significantly higher "straight rope" factors z_{si}^{T} than does the corresponding strand of the filler-wire rope, and, primarily because of the unusually large center wire of the Seale strand—see Fig. 3—the bending factor z_{si}^{B} for this wire greatly exceeds the largest of the bending factors of the filler-wire strand. Curves like the ones shown in Fig. 5 may also be constructed for the Seale rope; they tend to be more spread out vertically, indicating a less-optimum distribution of stresses among the various wires.

Conclusions

Linearized equations of equilibrium for helical wires and for helical strands of wires can be satisfied, along with appropriate compatibility conditions for wires within strands and for strands within the rope, in a manner that allows the strains, stresses, and generalized forces in all the wires and strands to be computed for ropes of complex cross section, including ropes with internal-wire-rope cores. The results may be extended by superposition to include the important case of loaded ropes pulled over a sheave or bent around a drum.

In this paper, results are given for certain Seale and filler-wire constructions and results could be generated for other constructions, such as the 6x31 Warrington-Seale, the 6x43 filler-wire Seale, and the 6x46 Seale filler-wire [30, p. 12].

Predicted values of the "effective modulus" are slightly higher than those given in the literature for IWRC ropes. The discrepancy is probably due to the failure to take into account the contact deformations arising from the internal point and line loads, and other possible interstitial movements afforded in actual ropes. The theory given in this paper would have to be modified slightly to treat in a realistic manner the deformation of ropes that *do not* have internal-wire-rope cores; the modification would concern the change in strand radius which, in this paper, was assumed to depend solely on Poisson contraction of the given strand and all the strands beneath it.

Acknowledgments

Valuable discussions with Mr. Eugene H. Skinner and Mr. Grant L. Anderson, P.E., of the U.S. Interior Department's Bureau of Mines, Spokane, are gratefully acknowledged. Much of the work reported here may be found in a recent report [32] to the Bureau of Mines on Contract J0100011 with the University of Illinois at Urbana-Champaign.

References

1 Suslov, B. M., "On the Modulus of Elasticity of Wire Ropes," *Wire and Wire Products*, Vol. 11, 1936, pp. 176-182.

2 Drucker, D. C., and Tachau, H., "A New Design Criterion for Wire Rope," *ASME Journal of Applied Mechanics*, Vol. 12, 1945, pp. A33-38.

3 Hall, H. M., "Stresses in Small Wire Ropes," *Wire and Wire Products*, Vol. 26, 1951, pp. 257-259.

4 Hruska, F. H., "Calculations of Stresses in Wire Rope," *Wire and Wire Products*, Vol. 26, 1951, pp. 766-767 and 799-801.

5 Hruska, F. H., "Radial Forces in Wire Ropes," *Wire and Wire Products*, Vol. 27, 1952, pp. 459-463.

6 Hruska, F. H., "Tangential Forces in Wire Ropes," *Wire and Wire Products*, Vol. 28, 1953, pp. 455-460.

7 Leissa, A. W., "Contact Streses in Wire Ropes," *Wire and Wire Products*, Vol. 34, 1959, pp. 307-314 and 372-373.

8 Starkey, W. L., and Cress, H. A., "An Analysis of Critical Stresses and Mode of Failure of a Wire Rope," *ASME Journal of Engineering for Industry*, Vol. 81, 1959, pp. 307-316.

9 Bert, C. W., and Stein, R. A., "Stress Analysis of Wire Rope in Tension and Torsion," *Wire and Wire Products*, Vol. 37, 1962, pp. 769-770.

10 Machida, S., and Durelli, A. J., "Response of a Strand to Axial and Torsional Displacements," *Journal of Mechanical Engineering Science*, Vol. 15, 1973, pp. 241-251.

11 Durelli, A. J., and Machida, S., "Response of Epoxy Oversized Models of Strands to Axial and Torsional Loads," *Experimental Mechanics*, Vol. 13, 1973, pp. 313-321.

12 Lutchansky, M., "Axial Stresses in Armor Wires of Bent Submarine Cables," *ASME Journal of Engineering for Industry*, Vol. 91, 1969, pp. 687-693.

13 Knapp, R. H., "Derivation of a New Stiffness Matrix for Helically Armoured Cables Considering Tension and Torsion," *International Journal for Numerical Methods in Engineering*, Vol. 14, 1979, pp. 515-529.

14 Huang, N. C., "Finite Extension of an Elastic Strand with a Central Core," *ASME Journal of Applied Mechanics*, Vol. 45, 1978, pp. 852-858.

15 Phillips, J. W., and Costello, G. A., "Contact Stresses in Twisted Wire Cables," *Journal of the Engineering Mechanics Division, ASCE*, Vol. 100, 1974, pp. 1096-1099.

16 Costello, G. A., and Phillips, J. W., "Contact Stresses in Thin Twisted Rods," *ASME Journal of Applied Mechanics*, Vol. 40, 1973, pp. 629-630.

17 Costello, G. A., and Phillips, J. W., "Effective Modulus of Twisted Wire Cables," *Journal of the Engineering Mechanics Division, ASCE*, Vol. 102, 1976, pp. 171-181.

18 Phillips, J. W., and Costello, G. A., "Axial Impact of Twisted Wire Cables," *ASME Journal of Applied Mechanics*, Vol 44, 1977, pp. 127-131.

19 Costello, G. A., and Sinha, S. K., "Static Behavior of Wire Rope," *Journal of the Engineering Mechanics Division, ASCE*, Vol. 103, 1977, pp. 1011-1022.

20 Costello, G. A., and Miller, R. E., "Lay Effect of Wire Rope," *Journal of the Engineering Mechanics Division, ASCE*, Vol. 105, 1979, pp. 597-608.

21 Costello, G. A., and Butson, G. J., "A Simplified Bending Theory for Wire Rope," *Journal of the Engineering Mechanics Division, ASCE*, Vol. 108, 1982, pp. 219-227.

22 Costello, G. A., "Stresses in Multilayered Cables," *ASME Journal of Energy Resources Technology*, Vol. 105, 1983, pp. 337-340.

23 Velinsky, S. A., Analysis of Wire Ropes with Complex Cross Sections, Ph.D. Thesis, University of Illinois at Urbana-Champaign, Department of Theoretical and Applied Mechanics, 1981, 87 pp.

24 Velinsky, S. A., Anderson, G. L., and Costello, G. A., "Wire Rope with Complex Cross Sections," *Journal of the Engineering Mechanics Division, ASCE*, Vol. 106, 1984, to appear.

25 Phillips, J. W., and Fotsch, P. D., "Preliminary Analysis of Filler-Wire Hoisting Rope," *Developments in Mechanics*, Vol. 12, 1983, pp. 397-400.

26 Love, A. E. H., *A Treatise on the Mathematical Theory of Elasticity*, Dover Publications,

New York, 1944, Chapters 18 and 19.

27 Timoshenko, S. P., *Strength of Materials, Part II*, 3rd ed., D. Van Nostrand, New York, 1956, pp. 295-298.

28 Costello, G. A., "Large Deflections of Helical Springs Due to Bending," *Journal of the Engineering Mechanics Division, ASCE*, Vol. 103, 1977, pp. 481-487.

29 McConnell, K. G., and Zemke, W. P., "The Measurement of Flexural Stiffness of Multistranded Electrical Conductors while Under Tension," *Experimental Mechanics*, Vol. 20, 1980, pp. 237-244.

30 *Wire Rope Users Manual*, American Iron and Steel Institute, Washington, 1979.

31 *Code of Federal Regulations*, U. S. Government Printing Office, Washington, Vol. 30 (Mineral Resources), 1980, Article 57.19-39.

32 Costello, G. A., and Phillips, J. W., "Stress Analysis of Wire Hoist Rope," Technical Report No. UILU-ENG 83-6006, Engineering Documents Center, University of Illinois at Urbana-Champaign, Urbana, Illinois, September 1983, 103 pp.

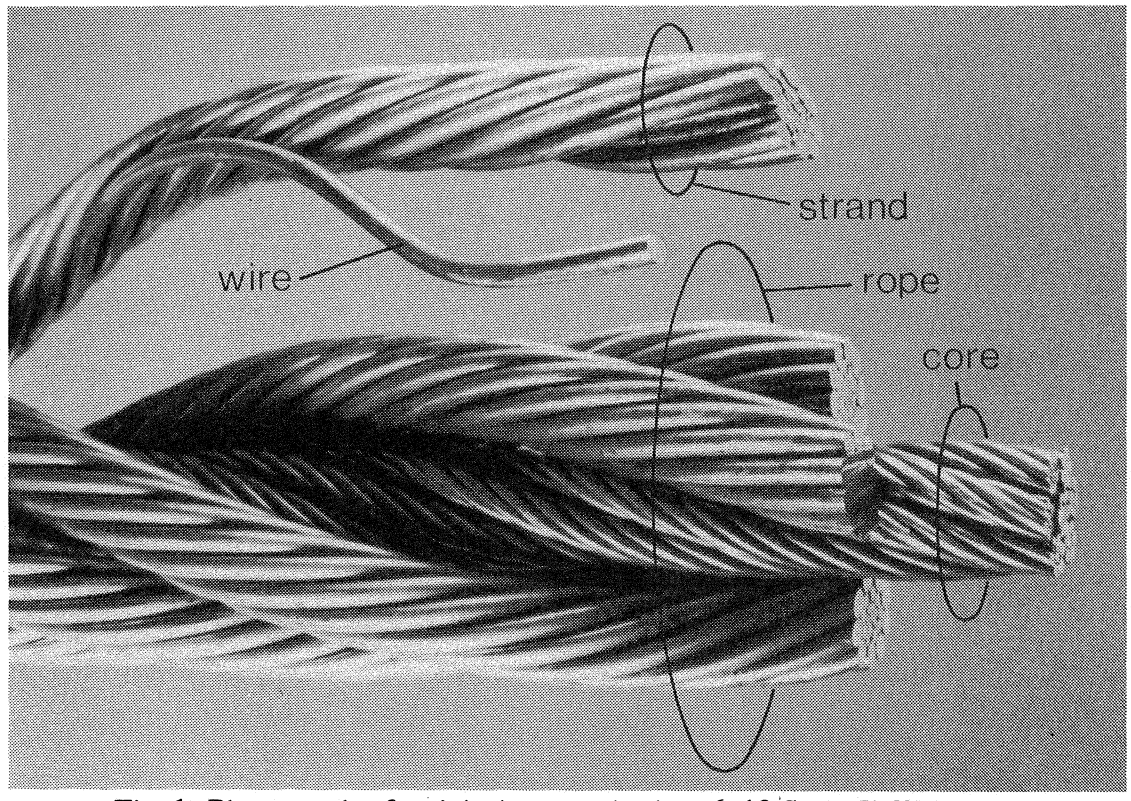

Fig. 1 Photograph of a right lay, regular lay, 6x19 Seale IRWC rope

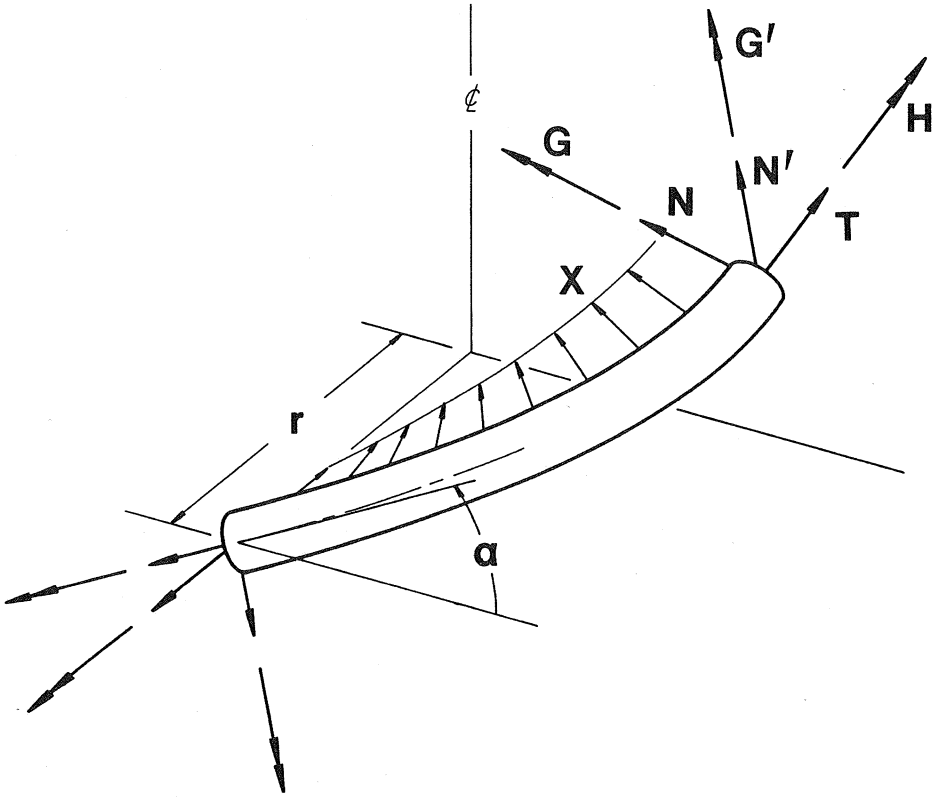

Fig. 2 Nomenclature for a wire or strand

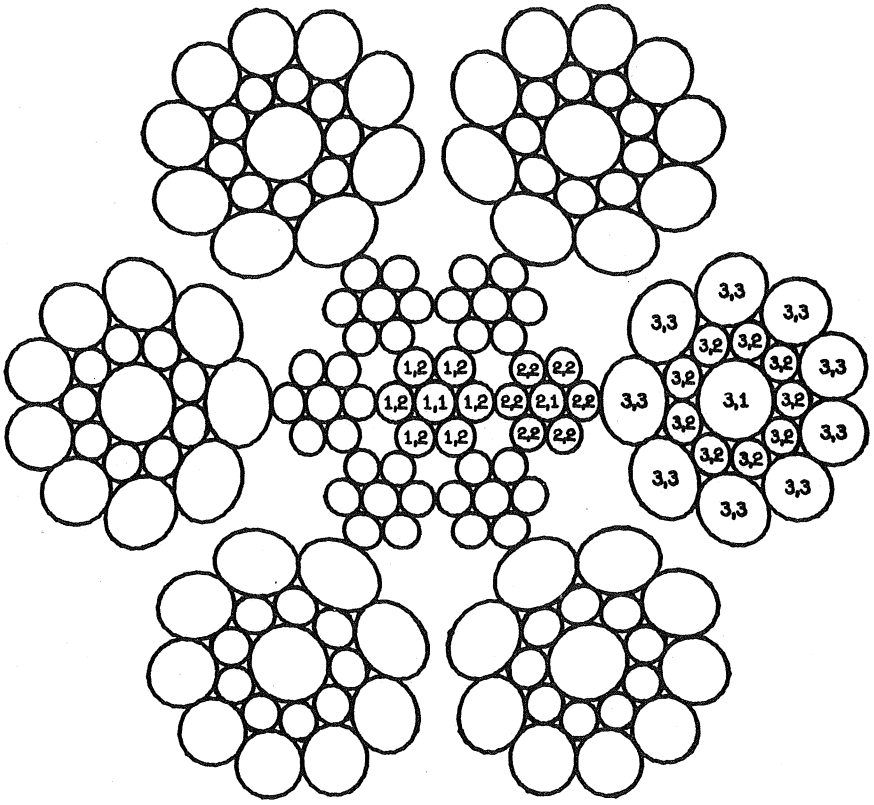

Fig. 3 Cross section of the 6x19 Seale IWRC. Wire cross sections are drawn in their "true" elliptical shape

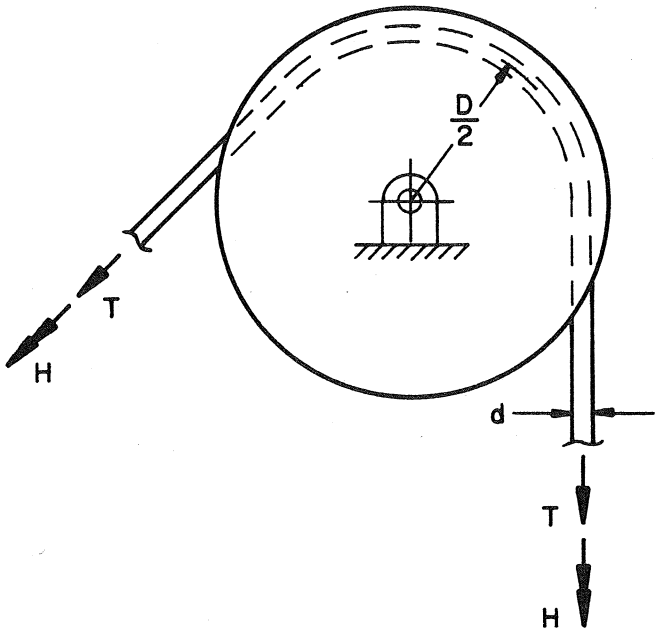

Fig. 4 Loaded rope passed over a sheave

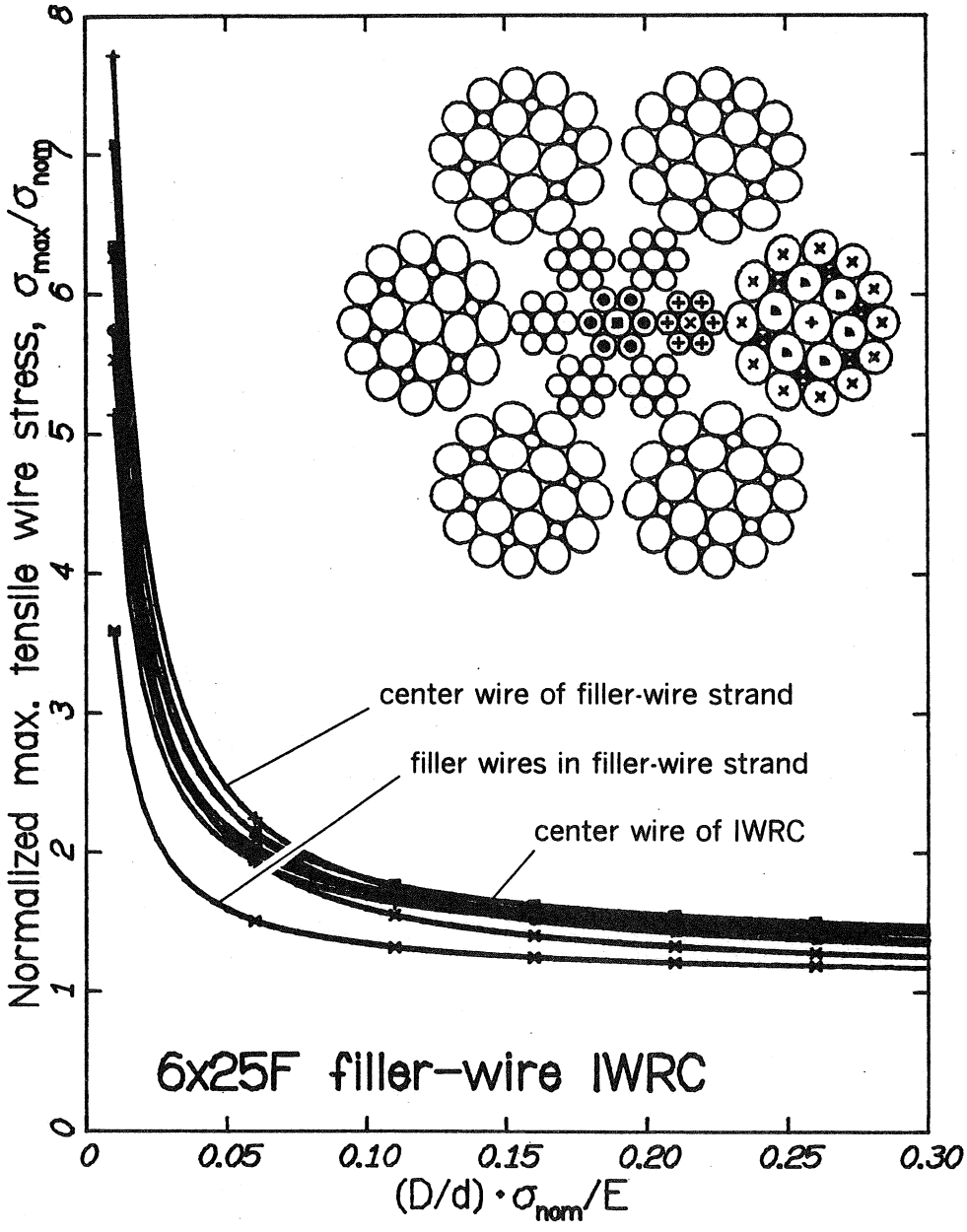

Fig. 5 Maximum tensile wire stresses in a 6x25 filler-wire IWRC as functions of the bending parameter $\frac{D}{d}\cdot\frac{\sigma_{nom}}{E}$.

Table 1 Geometrical data for the types of rope considered

Type of rope	Strand data					Wire data							
	Layer, s	No., m_s	Angle, α_s	Factors $t=$	η_{0st}	Layer, i	No., m_{si}	Angle, α_{si}	Radius, R_{si} (in.)*	Factors, η_{sij} $(j=1,\cdots,i)$ $j=1$	$j=2$	$j=3$	$j=4$
Solid rod	1	1	90.0°	1	1	1	1	90.0°	0.0316	0	–	–	–
1x7 strand	1	1	90.0°	1	1	1	1	90.0°	0.0316	0	–	–	–
						2	6	73.7°	0.0289	1	1	–	–
7x7, lang lay	1	1	90.0°	1	1	1	1	90.0°	0.0316	0	–	–	–
						2	6	73.7°	0.0289	1	1	–	–
	2	6	70.8°	1	1	1	1	90.0°	0.0277	0	–	–	–
				2	1	2	6	81.1°	0.0258	1	1	–	–
6x19 Seale IWRC, right lay regular lay	1	1	90.0°	1	1	1	1	90.0°	0.0316	0	–	–	–
						2	6	73.7°	0.0289	1	1	–	–
	2	6	70.8°	1	1	1	1	90.0°	0.0277	0	–	–	–
				2	1	2	6	81.1°	0.0258	1	1	–	–
	3	6	70.2°	1	1	1	1	90.0°	0.0573	0	–	–	–
				2	2	2	9	102.3°	0.0281	1	1	–	–
				3	1	3	9	111.2°	0.0499	$\cos(\pi/m_{32})$	η_{332}	$\cos\gamma$	–
	$\gamma=\sin^{-1}[((R_{31}+R_{32})/(R_{32}+R_{33}))\sin(\pi/m_{32})]$; $\eta_{332}=\cos(\pi/m_{32})+\cos\gamma$.												
6x25 filler-wire IWRC, left lay regular lay	1	1	90.0°	1	0	1	1	90.0°	0.0135	0	–	–	–
						2	6	83.5°	0.0120	1	1	–	–
	2	6	82.8°	1	1	1	1	90.0°	0.0115	0	–	–	–
				2	1	2	6	84.4°	0.0105	1	1	–	–
	3	6	109.7°	1	1	1	1	90.0°	0.0190	0	–	–	–
				2	2	2	6	80.0°	0.0175	1	1	–	–
				3	1	3	6	76.8°	0.0075	$\cos(\pi/m_{32})$	η_{332}	$\cos\gamma_1$	–
						4	12	72.1°	0.0160	η_{341}	η_{342}	η_{343}	$\cos\gamma_2$
	$\gamma_1=\sin^{-1}[((R_{31}+R_{32})/(R_{32}+R_{31}))\sin(\pi/m_{32})]$; $\eta_{332}=\cos(\pi/m_{32})+\cos\gamma_1$; $\gamma_2=\sin^{-1}[(r_{33}/(R_{33}+R_{34}))\sin(\pi/m_{34})]$, where $r_{33}=\eta_{331}R_{31}+\eta_{332}R_{32}+\eta_{333}R_{33}$; $\eta_{341}=\cos(\pi/m_{34})\eta_{331}$; $\eta_{342}=\cos(\pi/m_{34})\eta_{332}$; $\eta_{343}=\cos(\pi/m_{34})\eta_{333}+\cos\gamma_2$.												

* 1 inch = 25.4 mm

Table 2 Summary of generalized strains and loads in wires and strands of straight ropes, for an axial rope strain of 0.001 with no rope twist

Type of rope	Strand, s	Component	ϵ (10^{-6})	$\Delta\tau$ (in^{-1})*	$\Delta\kappa'$ (in^{-1})*	T (lbf)*	G' (lbf-in)*	H (lbf-in)*	N' (lbf)*	X (lbf/in)*	Rope factors z_{si}^T	z_{si}^B
Solid rod	1	—	1000†	0†	0	93.8	0	0	0	0	1.00	1.000
1x7 strand	1	Strand	1000†	0†	0	503	0	+6.84	0	0	—	—
		Wire 1	1000	0	0	93.8	0	0	0	0	1.13	0.353
		Wire 2	900	−0.00356	−0.00270	71.0	−0.045	−0.046	+0.139	−91.7	1.10	0.307
7x7, lang lay	1	Strand	1000	0	0	503	0	+6.84	0	0	—	—
		Wire 1	1000	0	0	93.8	0	0	0	0	1.25	0.127
		Wire 2	900	−0.00356	−0.00270	71.0	−0.045	−0.046	+0.139	−91.7	1.23	0.110
	2	Strand	864	−0.00134	−0.00127	371	−0.096	+2.38	+1.70	−234	—	—
		Wire 1	864	−0.00134	0	62.6	0	−0.014	0	0	1.13	0.104
		Wire 2	827	−0.00357	−0.00127	51.9	−0.013	−0.029	+0.025	−23.3	1.12	0.0953
	Rope		1000†	0†	—	2606	—	141.7	—	—	—	—
6x19 Seale IWRC, right lay regular lay	1	Strand	1000	0	0	503	0	+6.84	0	0	—	—
		Wire 1	1000	0	0	93.8	0	0	0	0	1.42	0.0483
		Wire 2	900	−0.00356	−0.00270	71.0	−0.045	−0.046	+0.139	−91.7	1.39	0.0420
	2	Strand	864	−0.00134	−0.00127	371	−0.096	+2.38	+1.70	−234	—	—
		Wire 1	864	−0.00134	0	62.6	0	−0.014	0	0	1.28	0.0395
		Wire 2	827	−0.00357	−0.00127	51.9	−0.013	−0.029	+0.025	−23.3	1.27	0.0362
	3	Strand	858	−0.00051	−0.00050	2260	−0.789	−94.54	−23.42	−590	—	—
		Wire 1	858	−0.00051	0	265.6	0	−0.100	0	0	1.26	0.0812
		Wire 2	817	+0.00141	−0.00078	60.6	−0.011	+0.016	−0.019	−32.0	1.21	0.0386
		Wire 3	741	+0.00094	−0.00113	174.0	−0.166	+0.107	−0.276	−149.0	1.17	0.0648
	Rope		1000†	0†	—	15317	—	1731	—	—	—	—
6x25 filler-wire IWRC, left lay regular lay	1	Strand	1000	0	0	96.7	0	+0.222	0	0	—	—
		Wire 1	1000	0	0	17.2	0	0	0	0	1.31	0.0503
		Wire 2	983	−0.00428	−0.00114	13.3	−0.0006	−0.0016	+0.0017	−6.8	1.31	0.0444
	2	Strand	980	−0.00170	−0.00050	72.0	−0.0011	+0.121	+0.0288	−15.9	—	—
		Wire 1	980	−0.00170	0	12.2	0	−0.0005	0	0	1.29	0.0424
		Wire 2	964	−0.00590	−0.00130	10.0	−0.0004	−0.0013	+0.0011	−4.4	1.29	0.0385
	3	Strand	857	+0.00122	−0.00121	410	−0.0410	+5.75	+3.46	−257	—	—
		Wire 1	857	+0.00122	0	29.1	0	+0.0029	0	0	1.15	0.0656
		Wire 2	831	−0.00259	−0.00116	24.0	−0.0026	−0.0044	+0.0083	−19.8	1.14	0.0593
		Wire 3	812	−0.00236	−0.00147	4.3	−0.0001	−0.0001	+0.0004	−4.6	1.09	0.0250
		Wire 4	777	−0.00195	−0.00182	18.7	−0.0028	−0.0023	+0.0090	−26.5	1.08	0.0519
	Rope		1000†	0†	—	2835	—	−120	—	—	—	—

* 1 in^{-1} = 39.37 m^{-1}; 1 lbf = 4.448 N; 1 lbf-in = 0.1130 N·m; 1 lbf/in = 175.1 N/m.
†Prescribed deformation of rope